Int. J. Electrochem. Sci., 15 **(2020)** 9902 – 9916, doi: 10.20964/2020.10.39

International Journal of
ELECTROCHEMICAL
SCIENCE
www.electrochemsci.org

A Thermodynamic Modelling Study of Aqueous Tetra-n-butyl Ammonium Halide Solutions

Li Sun[1,2,*], *Jierong Liang*[3]

[1] Department of Chemical and Biochemical Engineering, Technical University of Denmark, 2800, Kgs. Lyngby, Denmark
[2] College of Mechanical and Electrical Engineering, Hohai University, Changzhou 213022, People's Republic of China
[3] Department of Energy Conversion and Storage, Technical University of Denmark, 2800 Kgs. Lyngby, Denmark
[*]E-mail: lsun@kt.dtu.dk

Received: 10 June 2020 / *Accepted:* 7 August 2020 / *Published:* 31 August 2020

This work presents a novel model for aqueous electrolyte solutions that extends the Cubic Plus Association Equation of State by combining the Debye–Hückel theory for electrostatic interactions. This model is applied to perform a fluid phase modelling study of aqueous tetra-n-butyl ammonium halide solutions. The interaction parameters between cations/anions and water are evaluated by regression of the experimental mean ionic activity coefficients (MIAC) of the electrolyte. The results show that this novel model correlates reasonably well with the experimental MIAC (for example, the relative average deviations are 6.3% for the MIAC of tetra-n-butyl-ammonium bromide). The interaction parameters between cations/anions and gas are evaluated by regression of the experimental gas solubilities. The results show that this novel electrolyte model correlates reasonably well with gas solubility (for example, the relative average deviations are 2.9% for the nitrogen solubility in aqueous tetra-n-butyl-ammonium bromide solutions). For a more complete evaluation of the model, the electrostatic terms, parameter estimation approaches, and salting effects on gas solubility are analysed and discussed in detail.

Keywords: Aqueous Tetra-n-butyl Ammonium Halide Solutions; Electrolyte Equation of State; Debye–Hückel Theory; Hydrophobic Effect

1. INTRODUCTION

Special kinds of hydrates can be formed in the presence of certain additives (e.g., some quaternary ammonium salts). These formed hydrates are called semi-clathrate hydrates (SCH). The structures of SCH are more stable than those of normal hydrates.

In SCH, water (H_2O) molecules and the cations of additives are combined to build a clathrate, with the cations embedded in the framework cavities, while small guest gas (e.g., nitrogen (N_2), carbon dioxide (CO_2) and methane (CH_4)) molecules can be captured in small empty cages [1, 2].

Since SCH are stable even at atmospheric pressure, SCH attract attention because of their promising applications, including thermal storage, gas sequestration, and gas transportation [3, 4].

Pressure, temperature, and electrolyte molality determine the phase equilibrium conditions of SCH systems; phase modelling of SCH systems is developed by equating the fugacity of H_2O in the hydrate phase and the aqueous phase [5, 6]. Therefore, fluid-phase modelling is a critical part of hydrate-liquid-gas modelling. Thermodynamic models of electrolyte solutions have been developed by combining long-range electrostatic interactions with a model (i.e., Equations of State (EoS)) of short-range forces.

As the most common additives used to form SCH, tetra-n-butyl ammonium halides (TBAX) receive most attention [1-4, 7]. The models presented for TBAX fluid systems can be divided into two different approaches.

The φ-γ approach is the more common approach: among these models, the electrolyte Non-Random Two Liquid (e-NRTL) model [8] is the most used activity coefficient model.

In combination with e-NRTL, several models have been presented based on the Soave-Redlich-Kwong EoS (SRK) [9, 10], the Trebble–Bishnoi EoS (TB) [11, 12], and the Peng-Robinson EoS (PR) [13, 14]. Najibi and co-workers [15] combined the PR EoS [14] with "Mean Spherical Approximation including ionic hydration and association" [16] for aqueous solutions of tetra-n-butyl ammonium bromide (TBAB).

Contrasting the φ-γ models, the φ-φ approach uses an electrolyte EoS (e-EoS) to describe both the vapour and liquid phases. Relatively few e-EoS studies have been presented to date for TBAX systems. To the best of our knowledge, only three φ-φ models have been applied for TBAX fluid systems: "statistical associating fluid theory for potentials of variable range for electrolyte solutions" (SAFT-VRE) [17], modified Patel-Teja EoS (MPT) [18] and electrolyte Cubic Plus Association EoS (e-CPA) [19]. Paricaud [17] used SAFT-VRE to model TBAB fluid systems, and then, Fukumoto et al. [20] and Babu et al. [21] made improvements of SAFT-VRE and modelled some TBAX systems. In SAFT-VRE models, the interaction parameters between salt and H_2O are evaluated by the regression of the mean ionic activity coefficients (MIAC) of TBAX. Gas solubility is calculated from vapour-liquid flash calculations, and it should be noted that the effects of TBAB on the gas phase are negligible in their works [17, 20]. Ma et al. [22] applied MPT [18] to model aqueous solutions of TBAB and tetra-n-butyl ammonium fluoride (TBAF). In their modelling [22], the salt-H_2O interaction parameters and salt-gas interaction parameters were evaluated by the regression of MIAC and gas solubility in aqueous TBAB solutions, respectively. Sun et al. [23] modelled several TBAX fluid systems by using e-CPA [19]. In their works [23], the ions-H_2O and ions-gas interaction parameters were evaluated from the regression of MIAC and gas solubility in aqueous TABX solutions, respectively. Gas solubility is calculated using the vapour-liquid flash calculation in the work of Sun et al. [23], which is also extensively discussed the salting effects of TBAX.

To date, fluid phase modelling of H_2O+gas+TBAX systems has not been systematically studied, and limited e-EoS have been presented for such systems.

It is of interest to develop an e-EoS that is easy to use and has a relatively high modelling accuracy for TBAX systems. In this work, a novel e-EoS based on CPA [24] is presented for modelling aqueous TBAX solutions.

This contribution is divided into four parts: Section 2 presents the details of the novel e-EoS; Section 3 presents the parameter estimation; Section 4 presents the modelling results for both the binary and ternary systems; and Section 5 presents conclusions.

2. THERMODYNAMIC MODEL

An essential advantage of e-EoS is that it provides a consistent thermodynamic framework [25]. In this work, we try to develop an easy-to-use e-EoS that is suitable for industrial applications.

Hydrogen bonds form in liquid H_2O [26], and the CPA EoS [24] was presented as suitable for describing associating fluids. In CPA, the residual Helmholtz energy is from the physical term (A^{SRK}) and the association term (A^{Assoc}). There are five CPA pure-compound parameters: three SRK parameters and two association parameters (only for associating components). For mixtures, the classic vdw1f mixing rules are applied for the CPA co-volume parameters ($represented\ as\ b$) and the energy parameters [24].

In CPA, the residual Helmholtz energy for the physical term (the SRK EoS) [10] is calculated from:

$$A^{SRK} = nRT\left[-ln\left(1-\frac{b}{v}\right)-\frac{a(T)}{bRT}ln\left(1+\frac{b}{v}\right)\right] \quad (1)$$

where T is the temperature, R is the ideal gas constant, v is the molar volume, n is the number of moles present, and $a(T)$ is the temperature-dependent energy parameter of the mixture. b is calculated by:

$$b = \sum_i x_i b_i \quad (2)$$

where x_i is the mole fraction of component i (solvent, gas, ion) and b_i is the pure CPA co-volume parameter.

For a binary system without electrolyte, the classical vdw1f mixing rules are used for $a(T)$.

$$a(T) = \sum_i \sum_j x_i x_j \sqrt{a_i(T)a_j(T)}\left(1-k_{ij}\right) \quad (3)$$

The energy parameter of the mixture, $a_i(T)$ is given by:

$$a_i = a_{0i}\left(1+c_{1i}\left(1-\sqrt{T_{ri}}\right)\right)^2 \quad (4)$$

where T_{ci} is the critical temperature for component i and T_{ri} is the reduced temperature of component i, defined as $T_{ri} = T/T_{ci}$.

The association term A^{Assoc} is from Wertheim's association theory [27]:

$$A^{Assoc} = RT\left[\sum_i n_i \sum_{A_i}\left(\ln X_{A_i} - \frac{1}{2}X_{A_i} + \frac{1}{2}\right)\right] \quad (5)$$

$$\frac{1}{X_{A_i}} = 1 + \sum_j \rho_j \sum_{B_i} X_{B_j}\Delta_{A_iB_j} \quad (6)$$

where n_i is the number of moles of component i, ρ_j is the density of component j, X_{A_i} is the fraction of site A of component i that is not bonded to other sites, and $\Delta_{A_iB_j}$ is the association strength calculated by:

$$\Delta_{A_iB_j} = g(\rho)\left[\exp\left(\frac{\varepsilon^{A_iB_j}}{k_BT}\right) - 1\right] b_{ij}\beta^{A_iB_j} \quad (7)$$

where $\beta^{A_iB_j}$ is the association volume, $\varepsilon^{A_iB_j}$ is the association energy, and b_{ij} is given by $b_{ij} = (b_i + b_j)/2$, similar to Eq. (2). The radial distribution function is expressed as $g(\rho) = (1 - 1.9\eta)^{-1}$, with the packing fraction η defined as $b/4v$.

Long-range electrostatic forces between charged molecules should be considered to accurately describe the phase behaviour of systems containing electrolytes [25].

The "ion-ion+ion-H_2O" (II+IW) theory [28, 29] states that the basic electrostatic interactions in electrolyte solutions are ion-ion interactions and ion-H_2O interactions. Previous studies [28-30] on activity coefficients of individual ions show that both ion-ion and ion-H_2O interaction combinations are equally important.

Most e-EoS [17-19, 31-33] apply Debye-Hückel theory [34] or the mean spherical approximation (MSA) [35] for ion-ion interaction calculations. Maribo-Mogensen et al. [36] studied the performances of the nonrestricted primitive MSA [35] and Debye−Hückel [34]. The investigation showed that the performance of Debye−Hückel and the MSA are similar. They also concluded that the Debye−Hückel theory is simpler than the MSA and might be able to be applied in connection with EoS without a loss of accuracy. In our model, the Debye−Hückel theory is selected for calculations of electrostatic interactions.

The Born equation [37] is used for ion-H_2O interaction calculations in some thermodynamic models. However, other approaches are also presented for ion-H_2O interaction calculations. Fraenkel [38] presented an extension of the Debye-Hückel theory (DH−SiS) that considers the ion and the counter-ion with two shells of different ion sizes. Other scholars have also presented similar treatments, and some models [33] use the hydrated ionic diameter in electrostatic interaction calculations to account for the contribution of the ion-H_2O interaction.

In our model, we consider ion-H_2O interactions via adjusting the ion radius in the electrostatic calculations, i.e., we use the hydrated ionic radii.

After combining the Debye-Hückel theory with the physical term and association term, a novel e-EoS is developed, and the residual Helmholtz energy is given as:

$$A^{Res} = A^{SRK} + A^{Assoc} + A^{DH} \quad (8)$$

The contribution from the ion-ion interaction A^{DH} is calculated using the Debye-Hückel theory [34]:

$$A^{DH} = -\frac{k_BTV}{4\pi N_A \sum_i n_i Z_i^2}\sum_i n_i Z_i^2 \chi_i \quad (9)$$

Here, the function χ_i is given by:

$$\chi_i = \frac{1}{d_i^3}\left[\ln(1 + \kappa d_i) - \kappa d_i + \frac{1}{2}(\kappa d_i)^2\right] \quad (10)$$

where d_i is the hydrated ionic diameter of ion i and κ is the inverse Debye screening length given by:

$$\kappa = \left(\frac{e^2 N_A^2}{\varepsilon_r \varepsilon_0 RTV}\sum_{ions} n_i Z_i^2\right)^{1/2} \quad (11)$$

where V is total volume in m^3, N_A is the Avogadro constant, n_i is the number of moles of ion i, and Z_i is the charge of ion i, ε_0 is the permittivity in vacuum, ε_r is the relative static permittivity of the solvent.

The Huron-Vidal/NRTL mixing rule has additional flexibility to electrolyte systems [19]; for a binary system involving an ion:

$$\frac{a}{b} = \sum_i x_i \frac{a_i}{b_i} - \frac{g^{E,\infty}}{ln\,2} \tag{12}$$

$$\frac{g^{E,\infty}}{RT} = \sum_i x_i \frac{\sum_j x_j b_j \exp\left(-\alpha_{ji}\frac{\Delta U_{ji}}{RT}\right)\frac{\Delta U_{ji}}{RT}}{\sum_j x_j b_j \exp\left(-\alpha_{ji}\frac{\Delta U_{ji}}{RT}\right)} \tag{13}$$

where $g^{E,\infty}$ is the excess Gibbs energy at infinite pressure, α_{ji} is the NRTL non-randomness parameter, and ΔU_{ji} is the change in interaction energy between like and unlike interactions.

To improve the applicability of the model, the "ion-solvent" is converted into "cation/anion-solvent" ($\Delta U_{cation/anion-solvent}$), and the "ion-gas" is converted into "cation/anion-gas" ($\Delta U_{cation/anion-gas}$), which means that the interaction parameter $\Delta U_{cation-solvent}$ is equal to $\Delta U_{anion-solvent}$and $\Delta U_{cation-gas}$ is equal to $\Delta U_{anion-gas}$.

3. PARAMETER ESTIMATION

In this work, three TBAX+H_2O systems are studied: H_2O+TBAB, H_2O+tetra-n-butyl ammonium chloride (TBAC), and H_2O+TBAF. Moreover, three H_2O+gas+TBAX systems are studied: H_2O+CO_2+TBAB, H_2O+CH_4+TBAB, and H_2O+N_2+TBAB.

The CPA parameters of H_2O and the gases are from the literature [23, 24, 39] and are listed in Table 1.

Table 1. CPA parameters of the pure components.

Compound	b [L/mol]	Γ [K]	c_1	$\varepsilon^{A_iB_j}/R$ [K]	$\beta^{A_iB_j}$
H_2O [24]	0.014515	1017.34	0.6736	2003.25	0.0692
CO_2 [39]	0.0272	1551.222	0.7602	0	0
CH_4 [39]	0.02910	959.028	0.44718	0	0
N_2 [23]	0.02605	634.070	0.49855	0	0

In Table 1, b is the CPA co-volume parameter (in Eq. (1)), Γ is the CPA reduced energy parameter ($\Gamma = a_0/(Rb)$), and c_1 is the CPA alpha-function temperature-dependence (in Eq. (4)).

In this work, H_2O is set to a four-site (4C) scheme, and the three gases are set to non-association. The temperature-dependent H_2O-gas interaction parameters (k_{ij} in Eq. (3)) are from the literature (-0.15508+0.000877T [40], 0.8243-245.33/T [40], and 1.0741-368.3066/T [23] for H_2O-CO_2, H_2O-CH_4, and H_2O-N_2, respectively).

Ion size is a critical physical parameter in electrostatic interaction calculations. For the radii of Br^-, Cl^- and F^-, we used the Pauling radii (1.95 Å, 1.81 Å, and 1.36 Å for Br^-, Cl^- and F^-, respectively)

[41]. There are four soft and long hydrophobic alkyl chains on the TBA^+ cation, and the positive charge is sterically hindered by the alkyl substituents [42]. Sun et al. [42] investigated the effects of ion size on thermodynamic modelling performance and gave a value of the TBA^+ radius (2.25 Å), which was chosen in this work.

As discussed above, hydrated ionic radii are used in electrostatic interaction calculations. Because there is no experimental free hydration energy for some ions, to keep the model's universality, the empirical L-P-S equations [43] are used to estimate the hydrated radii:

$$r_{hyd.C} = r_{cation} + 0.85\ \text{Å} \quad (14)$$

$$r_{hyd.A} = r_{anion} + 0.1\ \text{Å} \quad (15)$$

In Eqs. (14) and (15), r_{cation} is the physical radius of TBA^+ (2.25 Å) and r_{anion} is the Pauling radius of the corresponding anion. $r_{hyd.C}$ and $r_{hyd.A}$ are the hydrated ionic radii.

The CPA co-volume parameter of ions can be estimated by [25]:

$$b = 2/3\pi N_A (2r_i)^3 \quad (16)$$

where r_i is the physical radius (r_{cation} in Eq. (14) and r_{anion} in Eq. (15)) of the ion *i*.

The ε_r is critical the electrostatic calculations [44]. By using infrared spectroscopy, Stangret and Gampe [45] found that the number of hydrogen bonds significantly increases in aqueous TBAX solutions. In other words, hydrophobic effects exist in aqueous TBAX solutions. The hydrophobic effects of TBAX can strengthen the hydrogen bonding of water, changing the H_2O structure around TBA^+, resulting in an increase of the ε_r [46].

There are limited experimental values of ε_r for aqueous TBAX solutions. In modelling research using SAFT-VRE and MPT, the ε_r of pure solvent has been used in electrostatic interaction calculations. In this work, the ε_r of pure H_2O is used in the electrostatic interaction calculations.

In this work, the cation/anion-solvent interaction parameters are evaluated by the regression of MIAC, and the cation/anion-gas interaction parameters are evaluated by the regression of gas solubility in aqueous phase.

The objective function of the regression is:

$$F = \sum_i^{Np} \left[\frac{x_i^{cal} - x_i^{exp}}{x_i^{exp}}\right]^2 \quad (17)$$

where *Np* is the number of experimental data points, x_i^{cal} represents the calculated values (MIAC of electrolyte and gas solubility), and x_i^{exp} represents the corresponding experimental values.

The results are presented as the relative average deviation:

$$RAD\% = \frac{1}{Np}\sum_i^{Np} \left|\frac{y_i^{cal} - y_i^{exp}}{y_i^{exp}}\right| \times 100\% \quad (18)$$

where y_i^{cal} is the calculated results of a given property (MIAC of electrolyte and gas solubility), and y_i^{exp} means the corresponding experimental data.

For each H_2O+TBAX binary system, there is only one adjustable parameter ($\Delta U_{cation/anion-solvent}$). After modeling the H_2O+TBAX binary system, there is only one adjustable parameter ($\Delta U_{cation/anion-gas}$) for each H_2O+gas+TBAX system.

4. RESULTS AND DISCUSSION

4.1 Binary Systems

First, the H_2O+TBAX systems were modelled. Binary systems containing H_2O+TBAX, were modelled using CPA in previous works [23, 40]. In this work, the H_2O+TBAB, H_2O+TBAC, and H_2O+TBAF systems are studied.

Table 2 and Figure 1 show the modelling results of the MIAC of TBAX in aqueous solution.

Table 2. Cation/anion-H_2O interaction parameters and modelling performance of the mean ionic activity coefficients of TBAX in aqueous solution.

Salt	$\Delta U_{cation/anion-water}$ [J/mol]	m [mol/kg]	RAD $\gamma_{\pm}^{m}$ [%]
TBAB [47, 48]	-785.1	0.1-6.0	6.3
TBAC [47]	-1318.3	0.1-6.0	6.0
TBAF [49]	-2167.7	0.1-1.6	4.9

In Table 2, $\Delta U_{cation/anion-water}$ is cation/anion-H_2O interaction parameters (from Eq. (13)), m is molality, and $\gamma_{\pm}^{m}$ is MIAC of TBAX.

From Table 2, it can be observed that our model overall correlates well the MIAC of TBAX in aqueous solution at reference temperature (298.15 K). Compared with the performance of other models, the performance of this work is worse than that of those using SAFT-VRE and similar to that of those using e-CPA. SAFT-VRE uses different cation radii for each electrolyte; additionally, in one SAFT-VRE modelling work [17], there were three interaction parameters for a single-electrolyte/single-H_2O system at reference temperature and another temperature-dependent parameter for wide temperature ranges. In Ma et al.'s work [22], there were four adjustable parameters for a single-electrolyte/single-H_2O system at reference temperature and no temperature-dependent parameter. Unfortunately, the reports using MPT did not give details of the modelling performance. In a e-CPA modelling work [42], there was only one adjustable parameter for a single-electrolyte/single-H_2O system at reference temperature and two extra temperature-dependent parameters for wide temperature ranges. In this work, there is only one interaction parameter, and temperature dependence is not considered.

It can be seen from Figure 1 that for a given electrolyte molality, the order of the values of MIAC are: TBAB<TBAC<TBAF. It is also observed that the absolute value of the interaction parameter between the cation/anion ration and H_2O is inversely proportional to ion radii of halides. This phenomenon may be explained in that smaller ion radii of halides cause large ions-H_2O interactions.

The experimental data of MIAC show the complex relationship of electrolyte molality. For the H_2O+TBAB system, the values decrease with increasing TBAB molality (at low to medium TBAB molality). For the H_2O+TBAC system, at low TBAC molality, the values of MIAC first decrease and then increase with increasing molality. After reaching maximum values, the MIAC of TBAC next decrease and then increase slightly. The values of the MIAC of TBAF in aqueous solution increase sharply with increasing TBAF molality. Wen and co-workers [49] explained that this phenomenon of TBAF could be attributed to the smaller radius of F^-, which may tend to immobilize H_2O around it due to its high charge density [49].

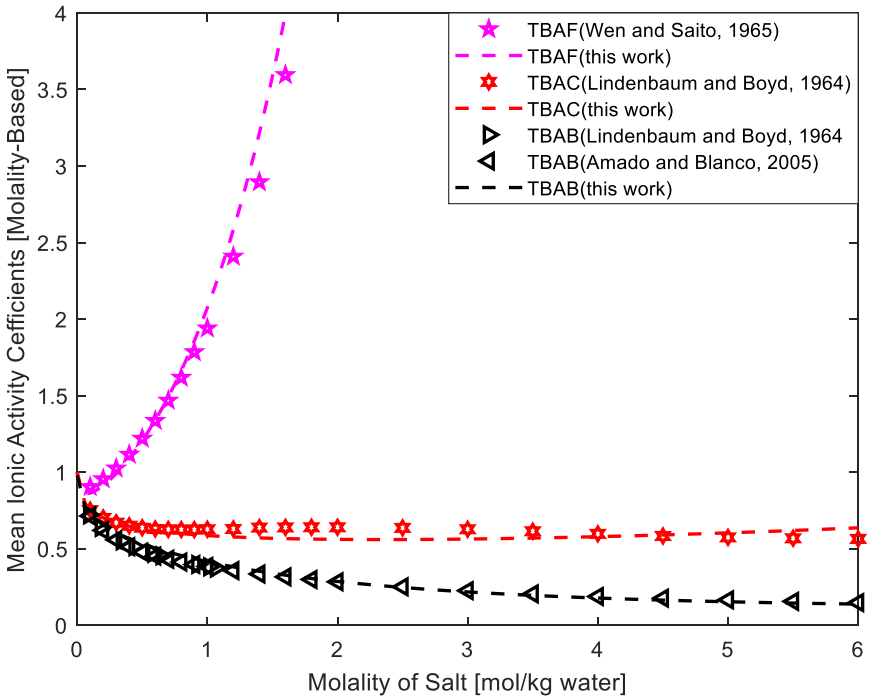

Figure 1. Mean ionic activity coefficients of TBAX in aqueous solution [47-49] at 298.15 K.

TBA^+ is large and hydrophobic; its size and hydrophobic effects help TBA^+ strengthen the "cage-like" H_2O structure [45]. The hydrophobic properties could be why the MIAC of TBAX shows an unexpected trend similar to that of common inorganic salts (e.g., NaCl).

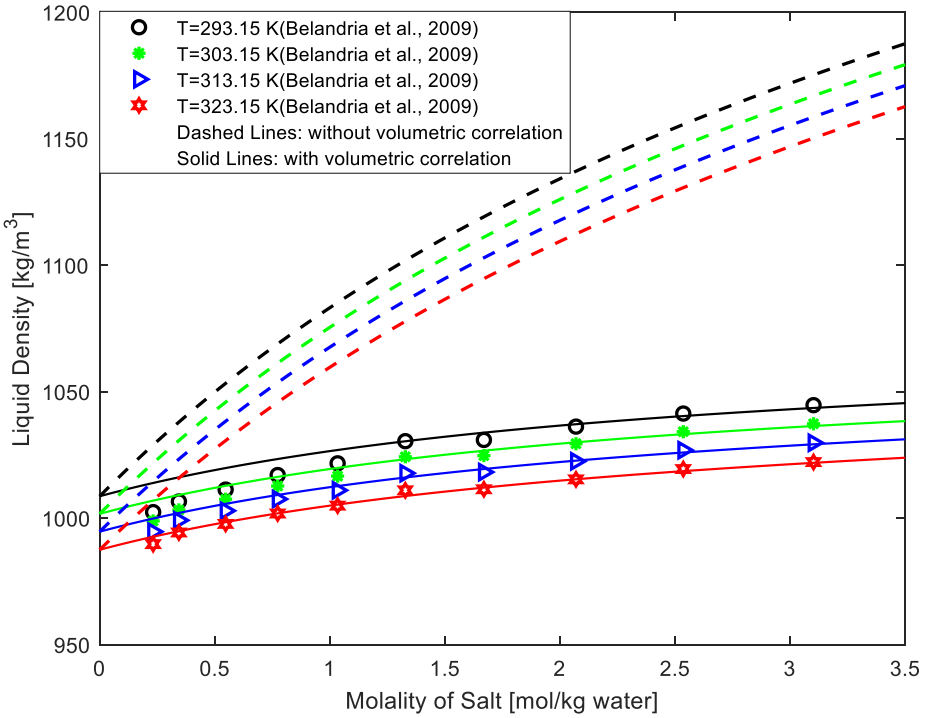

Figure 2. Densities of aqueous TBAB solutions [50] at different salt molalities and temperatures.

Liquid density is a critical property in industrial applications. Until now, only experimental densities of aqueous TBAB solution have been reported (with a narrow molality range) [50].

The modelling results shown in Figure 2 (dashed lines) show that this work overestimates the liquid densities of aqueous TBAB solution. In fact, other models also overestimate the liquid density of aqueous TBAB solution. In aqueous TBAX solutions, TBA^+ is large and has hydrophobic effects, so the existence of TBA^+ results in the formation of ice-like structures (with low density) of H_2O molecules around TBA^+ [17]. Both our model and prior models consider TBAX to be completely dissociated into ions in H_2O, and the hydrophobic effects are not included. Thus, these models may not be able to accurately represent this special phenomenon.

Here, we try to perform a volumetric correction of liquid densities. Since the deviations may come from the hydrophobic effects of TBA^+, we set a correlation parameter HV_{TBA} to improve the prediction ability of liquid densities:

$$v = v^{e-EoS} + x_{TBA} HV_{TBA} \quad (19)$$

where v^{e-EoS} is the calculated molar volume without correlation, x_{TBA} is the mole fraction of TBA^+, HV_{TBA} is the volumetric correction coefficient of TBA^+, and v is the molar volume of aqueous TBAX solutions. The volumetric correlation results (solid lines in Figure 2) show satisfactory agreement with experimental data (with RAD=0.6%). However, we can also see from Figure 2 that the correlation parameter does perform well for liquid densities at low TBAB molality and low temperature.

4.2 Ternary Systems

Hydrates have potential applications in gas sequestration and gas transportation [6]. CO_2 and N_2 are the main components of flue gas, and CO_2 can also be used as a displacement medium for CH_4 hydrate production [6]. Investigations of H_2O+gas (i.e., CO_2, CH_4, and N_2)+TBAX ternary systems are necessary for TBAX hydrate modelling.

Only experimental data of H_2O+gas+TBAB systems are available. Though experimental data for H2O+gas+TBAB are few, the accuracy of some datasets are doubtful. Here, we used the experimental data of H_2O+gas+TBAX systems that were selected in the previous work [23].

Before presenting the modelling results, it is necessary to review some related definitions and mechanisms. The gas solubility in liquid is defined as the maximum limit of gas that can be dissolved at a specified condition [51]. Gas solubility is easy to measure compared to the vapour phase, so most studies present gas solubility as vapour–liquid-equilibria data. CO_2, CH_4, and N_2 are not very soluble in H_2O. The two widely accepted mechanisms of gas dissolution are (1) the vacancy mechanism [52] (i.e., the gas filling of H_2O molecule interstices [52, 53]) and (2) the solvation mechanism [52] (i.e., the ion substitution for H_2O molecules in the structural framework of H_2O [52, 53]). The definitions of salting-in effects and salting-out effects are the increase and decrease of gas solubility due to the presence of electrolyte, respectively.

Table 3 and Figures 3 through 5 show the modelling results of gas solubility in aqueous TBAB solutions.

Table 3. Cation/anion-gas interaction parameters and modelling performance of gas solubility in aqueous TBAB solutions.

Gas	T [K]	P [MPa]	m [mol/kg]	$\Delta U_{cation/anion-gas}$ [J/mol]	RAD x_{gas} [%]
CO_2 [54, 55]	286.15-303.1	0.2-4.0	0.342-2.074	3920.2	7.4
CH_4 [56, 57]	278.15-308.15	0.101	0.096-4.01	4795.4	5.4
N_2 [58]	283.15-298.15	0.101	0-1.0	4987.6	2.9

In Table 3, $\Delta U_{cation/anion-gas}$ is the cation/anion-gas interaction parameters (from Eq. (13)), T is the temperature range, P is the pressure range, m is the molality range, and x_{gas} is gas solubility.

From Table 3, it can be observed that our model correlates well the gas solubility in aqueous TBAB solutions over wide electrolyte molality ranges, especially for N_2. The deviations for CO_2 are larger, with RAD greater than 7%. This result may be due to the deviations among the different experimental datasets [54, 55]. Among the published e-EoS modelling works, only a e-CPA modelling contribution [23] gave the performance details. The performance of our model is better than that of e-CPA. The difference in performance may mainly come from the different values of MIAC. e-CPA has two temperature-dependent adjustable parameters, but for these narrow temperature ranges, it seems that the temperature dependence of $\Delta U_{cation/anion-gas}$ can be ignored.

The solubility of gases in pure H_2O follow the sequence of $x_{CO_2}>x_{CH_4}>x_{N_2}$ at the same pressure and temperature [40]. It can be observed from Table 3 that the absolute values of $\Delta U_{cation/anion-gas}$ show the reverse order ($\Delta U_{cation/anion-CO_2}<\Delta U_{cation/anion-CH_4}<\Delta U_{cation/anion-N_2}$).

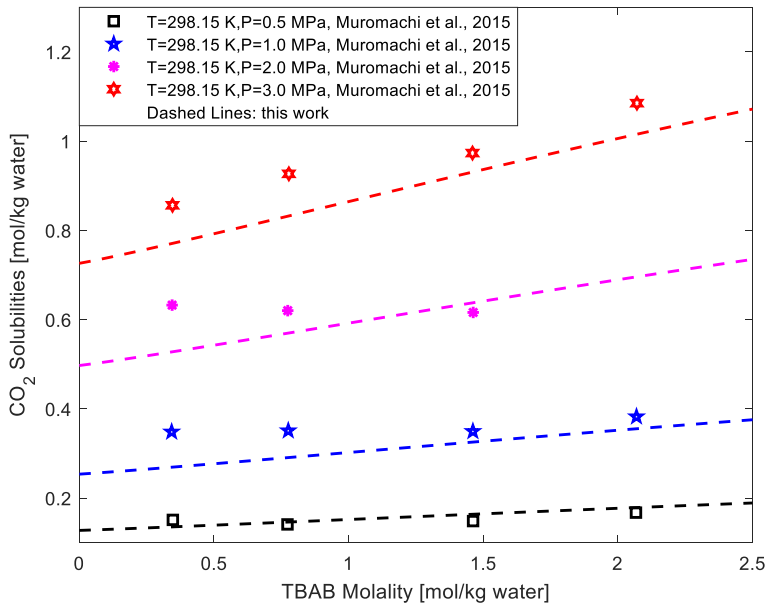

Figure 3. CO_2 solubility in aqueous TBAB solutions [55] at 298.15 K and different pressures.

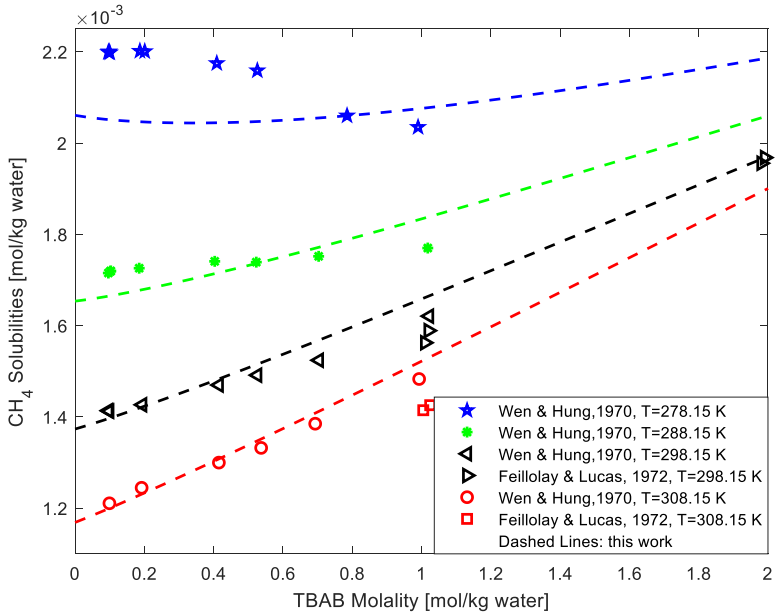

Figure 4. CH_4 solubility in aqueous TBAB solutions [56, 57] at atmospheric pressure and different temperatures.

Among H_2O+gas+TBAX systems, H_2O+CO_2+TBAB is the most studied. It can be observed from Figure 3 that our model correlates well with the CO_2 solubility in aqueous TBAB solutions. From Figure 3, we can also observe that the salting effects of TBAB on CO_2 solubility are complex. At different molalities and pressures, TBAB has different salting effects on CO_2. Lin and co-workers [54] stated that the salting effects of TBAB on CO_2 are different at different temperatures, pressures, and molalities. For the H_2O+CO_2+TBAB system, Lin and co-workers [54] noted that there is no clear region for salting-in or salting-out effects.

Unfortunately, some researchers [17, 20] did not consider the salting effects of TBAB on CO_2 solubility, i.e., they took the CO_2 solubility in aqueous TBAB solutions to be equal to that in pure H_2O at the same temperature and pressure [17].

From Figure 4, we can see that TBAB has complex salting effects on CH_4 solubility. TBAB has slight salting-out effects on CH_4 at lower temperatures (e.g., 278.15 K) but has significant salting-in effects on CH_4 at higher temperatures (e.g., 308.15 K). With increasing temperature, the salting-in effects become increasingly significant.

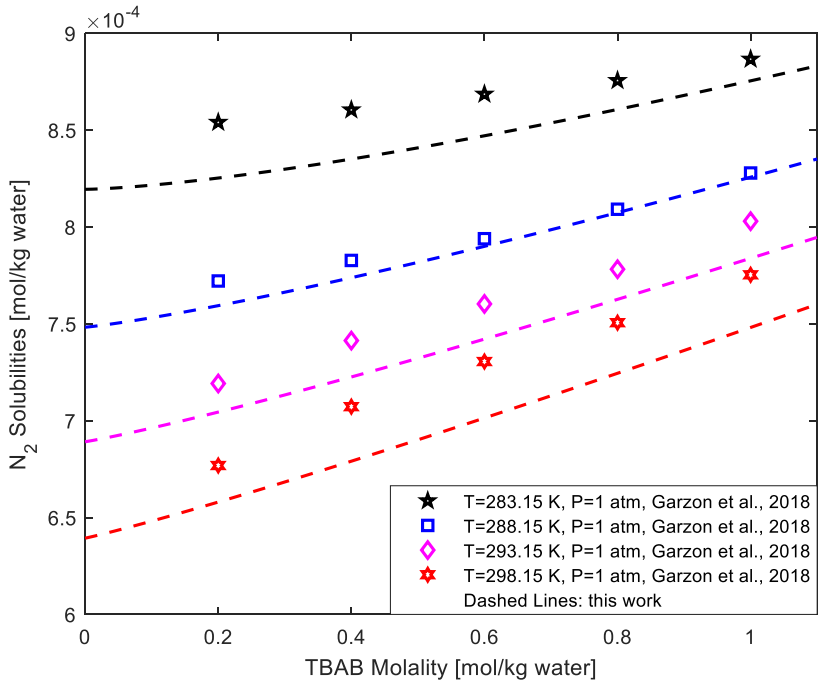

Figure 5. N_2 solubility in aqueous TBAB solutions [58] at atmospheric pressure and different temperatures.

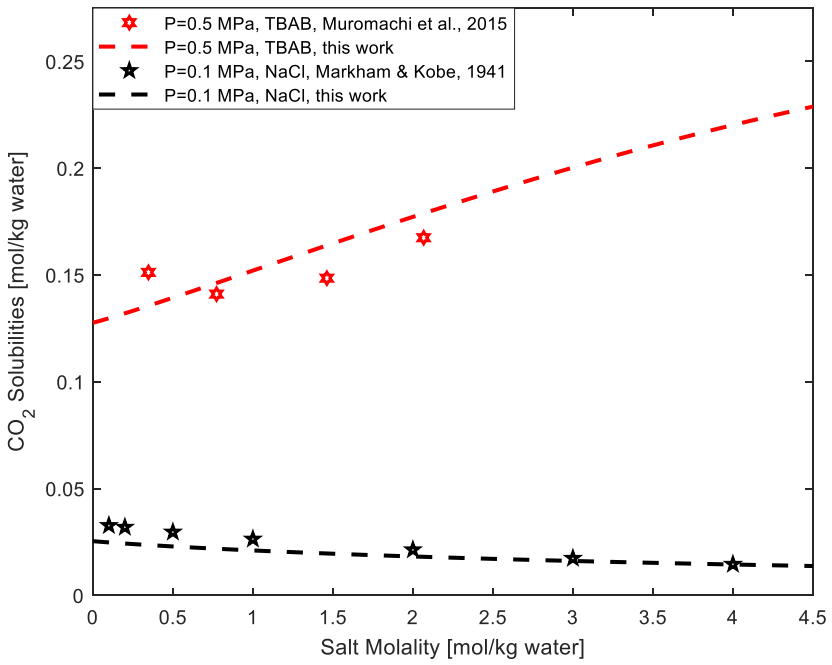

Figure 6. CO_2 solubility in aqueous solutions [55, 59] at 298.15 K and different pressures.

It can be seen from Figure 5 that TBAB has significant salting-in effects on N_2 solubility in H_2O, and the salting-in effects are more significant at higher temperatures (e.g., 298.15 K). Based on experimental data, Garzon et al. [58] noted that N_2 solubility increases as molality increases in a specific temperature-pressure-molality range (with molality=0.2-1.0 mol/kg, temperatures=283.15-298.15 K, and pressure=101.325 kPa).

TBAB has different salting effects on different gases in H_2O at low temperatures, i.e., salting-out effects on CH_4 and salting-in effects on N_2.

Figure 6 shows the comparison of CO_2 solubility in aqueous solutions of NaCl [59] and TBAB [55]. It can be clearly seen from Figure 6 that NaCl has significant salting-out effects on CO_2 solubility, while TBAB has significant salting-in effects on CO_2 solubility. Based on the mechanisms of gas dissolution mentioned above, the main reason for the salting-out effects of inorganic salts on gas solubility in H_2O is the formation of ion solvation, which reduces the number of interstices of H_2O and results in the escape of gas molecules from solution [60]. However, TBAB instead causes the salting-in of hydrophobic solutes under specific conditions, and some explanations for this effect [54, 56, 61] have been proposed. The acceptable explanations are as follows. (1) Anions (i.e., Br^-, Cl^- and F^-) and cations (TBA^+) form ion hydrations [56], which result in the salting-out effect of TBA^+ on gas, and this salting-out effect weakens with increasing temperature. (2) A "disorganization effect" [61] caused by the hydrophobic effect of TBA^+; this "disorganization effect" results in the salting-in effect, and this salting-in effect strengthens as the temperature and TBAX molality increase. The combination of these two opposite effects yields the salting effects of TBAB on gas solubility.

TBAB has significant salting effects on gas solubility, but many modelling works ignore the salting effects of TBAB [11, 17, 20] or consider the salting effects of TBAB to be relatively small [13]. None of the e-EoS modelling works (i.e., SAFT-VRE [17], MPT [22], and e-CPA [23]) and our model) do consider the hydrophobic effects of TBAB. Consequently, these models may not be able to accurately represent the "disorganization effect".

5. CONCLUSIONS

The salting effects of tetra-n-butyl ammonium halides on gas solubility in H_2O are complex at different temperatures and electrolyte molalities, and almost no explicit region of salting-in or salting-out effects is observed. The salting-in effects of tetra-n-butyl ammonium halides on gas solubility in H_2O tend to appear at relatively high temperatures and pressures. The hydrophobic effect of the tetra-n-butyl ammonium cation plays a significant role in phase behaviours.

This work presents a novel electrolyte model by extending the Cubic Plus Association Equation of State. This novel model applies Debye-Hückel theory to perform electrostatic interaction calculations. In the electrostatic interaction calculations, hydrated ionic radii are used to take ion-water interactions into account. Then, a modelling study for aqueous tetra-n-butyl ammonium halide solutions is presented.

The cation/anion-water interaction parameters are evaluated from the regression of the experimental mean ionic activity coefficients (MIAC) of tetra-n-butyl ammonium halide in aqueous solution, and the cation/anion-gas interaction parameters are evaluated from the regression of experimental gas solubility in aqueous solution. The results show that this model can correlate the MIAC of tetra-n-butyl ammonium halides reasonably well in aqueous solutions over wide electrolyte molality ranges. The model overestimates liquid densities.

This model considers tetra-n-butyl ammonium halides as strong electrolytes and does not take the hydrophobic effects of salts into account. Adding chemical equilibrium to this model is a potential enhancement for tetra-n-butyl ammonium halide systems in which hydrophobic effects exist.

ACKNOWLEDGEMENTS
The authors thank College of Mechanical and Electrical Engineering in Hohai University, Department of Chemical and Biochemical Engineering in Technical University of Denmark, and School of Energy and Power Engineering in Wuhan University of Technology for supporting this research.

References

1. G.A. Jeffrey, *Accounts of Chemical Research*, 2 (1969) 344.
2. R. McMullan, G.A. Jeffrey, *The Journal of chemical physics*, 31 (1959) 1231.
3. S.S. Fan, S.F. Li, J.Q. Wang, X.M. Lang, Y.H. Wang, *Energy & Fuels*, 23 (2009) 4202.
4. J. Deschamps, D. Dalmazzone, *Journal of thermal analysis and calorimetry*, 98 (2009) 113.
5. L.L. Shi, D.Q. Liang, *Fluid Phase Equilibria*, 386 (2015) 149.
6. J.E.D. Sloan, C.A. Koh, C. Koh, Clathrate hydrates of natural gases, *CRC press*, 1 (2007) 9.
7. D.L. Fowler, W.V. Loebenstein, D.B. Pall, C.A. Kraus, *Journal of the American Chemical Society*, 62 (1940) 1140.
8. C.C. Chen, H. Britt, J.F. Boston, L.B. Evans, *AIChE Journal*, 28 (1982) 588.
9. J.M. Herri, A. Bouchemoua-Benaissa, M. Kwaterski, A. Fezoua, Y. Ouabbas, A. Cameir˜ao, *Fluid Phase Equilibria*, 301 (2011) 171.
10. G. Soave, *Chemical engineering science*, 27 (1972) 1197.
11. J. Verrett, J.S. Renault-Crispo, P. Servio, *Fluid Phase Equilibria*, 388 (2015) 160.
12. M.A. Trebble, P.R. Bishnoi, *Fluid Phase Equilibria*, 35 (1987) 1.
13. A. Eslamimanesh, A.H. Mohammadi, D. Richon, *Chemical engineering science*, 81 (2012) 319.
14. D.Y. Peng, D.B. Robinson, *Industrial & Engineering Chemistry Fundamentals*, 15 (1976) 59.
15. H. Najibi, K. Momeni, M.T. Sadeghi, A.H. Mohammadi, *The Journal of Chemical Thermodynamics*, 87 (2015) 122.
16. J.P. Simonin, S. Krebs, W. Kunz, *Industrial & Engineering Chemistry Research*, 45 (2006) 4345.
17. P. Paricaud, *The Journal of Physical Chemistry B*, 115 (2011) 288.
18. Y.Y. Zuo, T.M. Guo, *Chemical engineering science*, 46 (1991) 3251.
19. B. Maribo-Mogensen, K. Thomsen, G.M. Kontogeorgis, *AIChE Journal*, 61 (2015) 2933.
20. A. Fukumoto, P. Paricaud, D. Dalmazzone, W. Bouchafaa, T.T.S. Ho, W. Fürst, *Journal of chemical & engineering data*, 59 (2014) 3193.
21. P. Babu, P. Paricaud, P. Linga, *Fluid Phase Equilibria*, 413 (2016) 80.
22. Q.L. Ma, J.L. Qi, G.J. Chen, C.Y. Sun, *Fluid Phase Equilibria*, 430 (2016) 178.
23. L. Sun, X.D. Liang, N.V. Solms, G.M. Kontogeorgis, *Fluid Phase Equilibria*, 507 (2020) 112423.
24. G.M. Kontogeorgis, E.C. Voutsas, I.V. Yakoumis, D.P. Tassios, *Industrial & Engineering Chemistry Research*, 35 (1996) 4310.
25. G.M. Kontogeorgis, G.K. Folas, Thermodynamic models for industrial applications: from classical and advanced mixing rules to association theories, *John Wiley & Sons*, 15 (2009) 463.
26. D.C. Rapaport, *Molecular Physics*, 50 (1983) 1151.
27. M.L. Michelsen, E.M. Hendriks, *Fluid Phase Equilibria*, 180 (2001) 165.
28. M. Valiskó, D. Boda, *The Journal of Physical Chemistry B*, 119 (2015) 1546.
29. M. Valiskó, D. Boda, *Molecular Physics*, 115 (2017) 1245.
30. L. Sun, X.D. Liang, N.V. Solms, G.M. Kontogeorgis, *Industrial & Engineering Chemistry Research*, 59 (2020) 11790.

31. A.H. Harvey, J.M. Prausnitz, *AIChE Journal*, 35 (1989) 635.
32. K. Aasberg-Petersen, E. Stenby, A. Fredenslund, *Industrial & Engineering Chemistry Research*, 30 (1991) 2180.
33. R. Sun, J. Dubessy, *Geochimica et Cosmochimica Acta*, 88 (2012) 130.
34. P. Debye, E. Hückel, *Physikalische Zeitschrift*, 24 (1923) 185.
35. J.L. Lebowitz, J.K. Percus, *Physical Review*, 144 (1966) 251.
36. B. Maribo-Mogensen, G.M. Kontogeorgis, K. Thomsen, *Industrial & Engineering Chemistry Research*, 51 (2012) 5353.
37. M. Born, *Zeitschrift für Physik*, 1 (1920) 45.
38. D. Fraenkel, *The Journal of Physical Chemistry B*, 116 (2012) 3603.
39. I. Tsivintzelis, G.M. Kontogeorgis, M.L. Michelsen, E.H. Stenby, *Fluid Phase Equilibria*, 306 (2011) 38.
40. L. Sun, G.M. Kontogeorgis, N.V. Solms, X.D. Liang, *Industrial & Engineering Chemistry Research*, 58 (2019) 17555.
41. L. Pauling, The Nature of the Chemical Bond, *Cornell university press Ithaca*, 5 (1960) 260.
42. L. Sun, X.D. Liang, N.V. Solms, G.M. Kontogeorgis, *Fluid Phase Equilibria*, 486 (2019) 37.
43. W.M. Latimer, K.S. Pitzer, C.M. Slansky, *Journal of Chemical Physics*, 7 (1993) 108.
44. J.L. Burgot, The notion of activity in chemistry, *Springer International Publishing*, 5 (2017) 35.
45. J. Stangret, T. Gampe, *The Journal of Physical Chemistry B*, 103 (1999) 3778.
46. R.W. Gurney, Ionic processes in solution, *Mcgraw-Hill*, 2 (1953) 54.
47. S. Lindenbaum, G.E. Boyd, *The Journal of Physical Chemistry*, 68 (1964) 911.
48. E. Amado, L.H. Blanco, *Fluid Phase Equilibria*, 233 (2005) 230.
49. W.Y. Wen, S.J. Saito, C.M. Lee, *The Journal of Physical Chemistry*, 70 (1966) 1244.
50. V. Belandria, A.H. Mohammadi, D. Richon, *The Journal of Chemical Thermodynamics*, 41 (2009) 1382.
51. M. Silberberg, Principles of general chemistry, *McGraw-Hill*, 3 (2012) 71.
52. A.F. Borina, O.Y. Samojlov, *Zhurnal Strukturnoj Khimii*, 15 (1974) 395.
53. M.S. Jhon, H. Eyring, Y.K. Sung, *Chemical Physics Letters*, 13 (1972) 36.
54. W. Lin, D. Dalmazzone, W. Fürst, A. Delahaye, L. Fournaison, P. Clain, *Journal of chemical & engineering data*, 58 (2013) 2233.
55. S. Muromachi, A. Shijima, H. Miyamoto, R. Ohmura, *The Journal of Chemical Thermodynamics*, 85 (2015) 94.
56. W.Y. Wen, J.H. Hung, *The Journal of Physical Chemistry*, 74 (1970) 170.
57. A. Feillolay, M. Lucas, *The Journal of Physical Chemistry*, 76 (1972) 3068.
58. L.C.A. Garzon, A.F. Suarez, C.M. Romero, *The Journal of Chemical Thermodynamics*, 126 (2018) 105.
59. A.E. Markham, K.A. Kobe, *Journal of the American Chemical Society*, 63 (1941) 449.
60. P.J. Carvalho, L.M.C Pereira, N.P.F. Gonçalves, A.J. Queimada, J.A.P. Coutinho, *Fluid Phase Equilibria*, 388 (2015) 100.
61. B. Hribar-Lee, K.A. Dill, V. Vlachy, *The Journal of Physical Chemistry B*, 114 (2010) 15085.